JOURNAL OF COMPUTATIONAL PHYSICS 68, 66–88 (1987)

A Comparative Study of Pseudo and Quasi Random Sequences for the Solution of Integral Equations

P. K. SARKAR

Health Physics Unit, Variable Energy Cyclotron Centre, I/AF Bidhan Nagar, Calcutta-700064, India

AND

M. A. PRASAD

Division of Radiological Protection, Bhabha Atomic Research Centre, Trombay, Bombay-400085, India

Received March 19, 1985; revised March 21, 1986

A numerical study for the solution of integral equations using random numbers from congruential generators and the Halton and the Faure sequences is presented. The results indicate that for high-precision Monte Carlo, quasi random sequences yield better results, in general. The relative performance of the quasi random sequences is better with Monte Carlo schemes which reduce the dimensionality of the problem. © 1987 Academic Press, Inc.

1. INTRODUCTION

The solution of integral equations are often estimated using simulated random walks, as, for example, in radiation transport problems [1]. The random sequences that are generally used for such simulations arise from congruential pseudo random numbers and are known as pseudo random sequences (PRS). However, as has been pointed out [2], these sequences suffer from the following disadvantages:

(a) for a finite sequence of length N, the rate of convergence is rather slow;

(b) they show poor lattice distribution properties especially in high dimensions.

Because of this unsatisfactory lattice distribution property, Marsaglia [3] insisted that for precision Monte Carlo work, congruential generators should not be used. Niederreiter [4], however, criticized Marsaglia's verdict by doubting the credentials of the lattice test as a meaningful statistical test. However, he also recommended the use of quasi random sequences (QRS) since the QRS have an asymptotically better rate of convergence. From a survey of the literature, it appears that the theoreticians prefer QRS, whereas the practitioners still prefer PRS

0021-9991/87 $3.00

because of the fact that for most of the practical problems solved the performance of PRS has been remarkably good. In a situation like this, a judicious choice of a sequence for a particular problem can be made only after carrying out numerical studies on problems where the solution is exactly known.

Studies carried out with test multidimensional integrals indicate better convergence with QRS [2]. This is because the upper bound of the error for integrals evaluated by uniformly distributed sequences is given by $T_N W(f)$ or $D_N V(f)$, where T_N and D_N are respectively the root mean square and extremal discrepancies of the sequence [5]. $W(f)$ and $V(f)$ depend on the function f to be integrated and can be said to describe the amount of variation in this function. This upper bound is valid only for functions which are of bounded variation in the sense of Hardy and Krause (BVHK) [4]. For quasi random sequences

$$T_N \leqslant C_s \frac{(\log N)^s}{N}, \tag{1}$$

where C_s is a constant depending on the sequence as well as the dimension s. On the other hand, for a random sequence, the expectation value of T_N is given by

$$T_N = \left(\frac{(1/2)^s - (1/3)^s}{N} \right)^{1/2}. \tag{2}$$

The congruential PRS is expected to follow this trend closely. It is evident that for sufficiently large N, QRS will give smaller error than PRS. For integral equations, Hua and Wang [6] have shown that the order of error one might expect with QRS is similar to that obtained for integrals.

It may be pointed out here that $T_N W(f)$ or $D_N V(f)$ give only upper bounds of the error and theoretical estimates of them are orders of magnitude larger than the true errors. Also, for problems involving large dimensions, numerical estimation of the discrepancy as well as the variation of the function are rather difficult and time consuming.

In this paper, we describe a numerical study to compare the relative merits of PRS and QRS in solving integral equations with the help of simulated random walks. The problem chosen for the present study yields to closed form solutions rather easily and at the same time approximates realistic particle transport rather closely. Specifically, the following two cases were studied:

(i) transmission through a one-dimensional finite slab with scattering only in the forward direction;

(ii) transmission and reflection in a one-dimensional finite slab with scattering in the forward and backward directions only.

2. Description of the Sequences

(i) *Congruential Pseudo Random Sequence*

A set of numbers which pass some specified statistical test for randomness are known as pseudo random numbers [4]. The commonly used sequence of pseudo random numbers, called the congruential pseudo random numbers in the unit interval [0, 1], may be generated as follows: let $m \geqslant 2$ be an integer. Generate a sequence (Y_n), $n = 0, 1, \ldots$, of integers in the least residue system modulo m using the recursion $Y_{n+1} = \lambda Y_n + r \pmod{m}$, with Y_0 an integer satisfying $0 \leqslant Y_0 \leqslant m$ and λ a positive integer relatively prime to m. Then the sequence (X_n), $n = 0, 1, \ldots$, where $X_n = Y_n/m$, is a sequence of congruential pseudo random numbers provided the parameters m, λ, Y_0 and r are chosen so that the sequence will pass the test for randomness.

A great deal of work has been done on finding optimum values for the parameters m, λ, r and Y_0 (see, for example, [4, 7]). m is usually selected in accordance with the machine capabilities, and it is known that r has only a secondary influence on the behaviour of the PRS, so that the properties of the sequence are mainly governed by the choice of the multiplier λ. In the present work, we have studied three different PRS, which have been designated PRS $-$ 1, PRS $-$ 2 and PRS $-$ 3, respectively. The parameters for these three sequences are

$$\begin{aligned} &\text{PRS} - 1: m = 2^{31}, \quad r = 0, \quad \lambda = 65539 \\ &\text{PRS} - 2: m = 2^{30}, \quad r = 1, \quad \lambda = 410092949 \\ &\text{PRS} - 3: m = 2^{32}, \quad r = 1, \quad \lambda = 1812433253. \end{aligned}$$

Y_0 in all the cases was taken as 3115. PRS $-$ 1 was available as a subroutine with a Morse code used for solving problems in neutron and gamma transport. PRS $-$ 2 and PRS $-$ 3 were taken from Borosh and Niederetter [7], in which the multipliers λ have been chosen such that they are optimal with respect to statistical independence of successive pairs of pseudo random numbers. The multidimensional PRS used in the present work were obtained as follows:

$$X_n^k = X_{s(n-1)+k}, \qquad 1 \leqslant k \leqslant s.$$

(ii) *Halton Sequence*

A class of infinite sequence in an s-dimensional unit cube has been introduced by Halton [5, 8]. This sequence is defined as follows. Let $p_1, p_2, \ldots, p_s$ be s integers which are relatively prime to each other. Also, let $a_i^{(k)}(n)$ be the p_k-adic expansion of $n-1$, where n is a positive integer, i.e.,

$$n - 1 = \sum_{i=0}^{\infty} a_i^{(k)}(n)(p_k)^i,$$

and let X_n^k be defined as

$$X_n^k = \sum_{i=0}^{\infty} a_i^{(k)}(n)\, p_k^{-i-1}, \qquad 1 \leqslant k \leqslant s.$$

The s-dimensional Halton sequence is then defined as the set of points $X_n^1, X_m^2, \ldots, X_n^s$, $n = 1, 2, \ldots$. The discrepancy of this class of sequences satisfies the inequality [9]

$$D_N^* \leqslant C_s \frac{(\log N)^s}{N} + O\left(\frac{(\log N)^{s-1}}{N}\right), \tag{3}$$

where

$$C_s = \prod_{k=1}^{s} \frac{p_k - 1}{2 \log p_k}. \tag{4}$$

In the present study, we have taken $p_1, p_2, \ldots, p_s$ as the first s primes.

Closely related to the Halton sequence are the scrambled Halton sequences defined as

$$S_n^{(k)} = \sum_{i=0}^{\infty} \sigma_i^{(k)}\left[a_i^{(k)}(n)\right] p_k^{-i-1},$$

where $\Sigma^k = (\sigma_i^{(k)})_{i \geqslant 0}$ is a set of permutations on the ensemble $(0, 1, 2, \ldots, p_k - 1)$. The permutations Σ^k are obtained in such a manner as to reduce the constant C_1 in Eq. (3) as far as possible (this constant corresponds to the one-dimensional discrepancy obtained with the integer p_k). It is expected that the multidimensional discrepancy would also decrease with the use of these permutations. In this work, we used the set of permutations suggested by Faure [10, 11].

(iii) *Faure Sequence*

A class of infinite sequences in an s-dimensional unit cube for $s \geqslant 2$, related to q-adic expansions of integers has been introduced by Faure [9]. This sequence is defined as follows: let q be a prime with $q \geqslant s \geqslant 2$. Let $\Sigma_i a_i(n)\, q^i$ be the q-adic expansion of $n-1$, where n is a positive integer. Let,

$$\begin{aligned} X_n^k &= \sum_{i=0}^{\infty} a_i(n)\, q^{i-1}, && k = 1 \\ &= \sum_{j=0}^{\infty} b_j\, q^{-j-1}, && 2 \leqslant k \leqslant q \\ b_j &= \left[\sum_{i \geqslant j} (k-1)^{i-j} \binom{i}{j} a_i(n)\right] && (\text{mod } q) \end{aligned}$$

with $\binom{i}{j} = i!/(i-j)!\,j!$.

Now, let $r_1,..., r_s$ be s distinct integers with $1 \leqslant r_i \leqslant q$ for each $1 \leqslant i \leqslant s$. The s-dimensional Faure sequence is then defined to be the set of points $X_n^{(r_1)} \cdots X_n^{(r_s)}$, $n = 1, 2,....$ In our work we have taken $r_1 = 1$, $r_2 = 2,..., r_s = s$.

The discrepancy D_N^* of this class of sequences satisfies the inequality

$$D_N^* \leqslant C_s \frac{(\log N)^s}{N} + O\left(\frac{(\log N)^{s-1}}{N}\right), \tag{5}$$

where

$$C_s = \frac{1}{s!}[(q-1)/(2 \log q)]^s, \qquad s \geqslant 3 \tag{6}$$

if q is a prime with $q \geqslant s \geqslant 2$. The bounds here have the important property that $C_s \to 0$ for $s \to \infty$ if q is the smallest prime $\geqslant s$.

In the present study, the Faure sequence was used in two different ways: In the first method, all the integrals associated with a problem were evaluated using a single sequence, which was generated using the smallest prime q larger than the largest dimensional integral associated with the problem. This procedure designated Faure-1 is similar to that used with PRS. In the second method, designated as Faure-2, a number of different sequences were generated with different primes, each integral being evaluated with the sequence generated with the smallest prime larger than the dimension of that integral.

3. Description of the Problem

For the purpose of the present study, we have chosen a one-dimensional homogeneous slab of finite thickness d with constant total and scattering cross sections Σ and Σ_s, respectively. The source is a plane parallel beam of particles incident normally on one surface of the slab.

Problem A

In the first problem, we consider the case when a particle after scattering travels in the same direction as the incident one. This problem was solved in two ways. The first scheme, A(1), follows analog Monte Carlo procedure, where,

(i) the distance x to the next collision site is chosen by sampling from the distribution $\Sigma \exp(-\Sigma x)$;

(ii) a score of 1 is given when the collision site lies beyond the boundary of the slab;

(iii) the particle survives the collision with probability Σ_s/Σ otherwise it is absorbed;

(iv) the history is terminated whenever the particle travels beyond the boundary of the slab or is absorbed.

The integral equation for the expectation value of the score $M_1(x)$ for a particle at x can be written as

$$M_1(x) = \int_x^d dx' \, \Sigma_s \exp[-\Sigma(x'-x)] \, M_1(x') + \exp[-\Sigma(d-x)]. \tag{7}$$

This can be readily solved to yield

$$M_1(x) = \exp[-(\Sigma - \Sigma_s)(d-x)]. \tag{8}$$

This Monte Carlo scheme simulates the solution of Eq. (4) by a Neumann series

$$\begin{aligned} M_1(x_0) &= \sum_{i=0}^{\infty} M_1^i(x_0) \\ &= \exp[-\Sigma(d-x_0)] + \sum_{i=1}^{\infty} \int_{x_0}^d dx_1 \int_{x_1}^d dx_2 \cdots \int_{x_{i-1}}^d dx_i \\ &\quad \times \left[\prod_{j=i}^{i} \Sigma_s \exp\{-\Sigma(x_j - x_{j-1})\} \right] \exp[-\Sigma(d-x_i)]. \end{aligned} \tag{9}$$

The nth term of the series indicates the mean contribution to the score by particles which have undergone n collisions and can be eaily obtained as

$$M_1^n(x_0) = \frac{[\Sigma_s(d-x_0)]^n}{n!} \exp[-\Sigma(d-x_0)]. \tag{10}$$

In a random walk simulation, the Neumann series described by Eq. (6) is evaluated using an s-dimensional sequence $R_m^s = (R_{1m}, R_{2m}, \ldots, R_{sm})$, $m = 1, 2, \ldots, N$; where N denotes the total number of histories used for the evaluation. For such a case, the ith term in Eq. (6) can be written as

$$\begin{aligned} M_1^i(x_0) &= \int_0^1 dR_1 \int_0^1 dR_2 \cdots \int_0^1 dR_{2i+1} \prod_{j=1}^{i} [\theta(\Sigma_s/\Sigma - R_{2j})] \\ &\quad \times \theta\left(\prod_{k=1}^{i} R_{2k-1} - \exp[-\Sigma(d-x)] \right) \theta\left(\exp[-\Sigma(d-x)] - \prod_{k=1}^{i+1} R_{2k-1} \right) \\ &= \int_0^1 dR_1 \int_0^1 dR_2 \cdots \int_0^1 dR_{2i+1} \, F_i(R_1, R_2, \ldots, R_{2i+1}). \end{aligned} \tag{11}$$

Here,

$$\begin{aligned} \theta(x) &= 0, \qquad x < 0 \\ &= 1, \qquad x > 0. \end{aligned}$$

It may be noted here that the infinite series given by Eq. (6) was terminated after a suitable number of terms since the Faure sequence requires predefined dimensionality for its generation. Care was taken, however, to ensure that the error due to truncation was negligible. The Monte Carlo estimate I_N of $I = M_1(0)$ from N histories is therefore

$$I_N = \frac{1}{N} \sum_{m=1}^{N} \sum_{i=1}^{K/2} F_i(R_m^{2i+1}), \tag{12}$$

where $K/2$ is the number of collisions at which the particle history is terminated. The relative error is defined by the relation $(I_N - I)/I$.

In the second scheme, A(2), to solve the same problem, the particles were not allowed to leave the system or to get absorbed. An expectation estimator was used for the scoring. The scheme is as follows

(i) the particle starts with a statistical weight $W = 1$;

(ii) a score $W \exp(-\Sigma d')$ is given, where d' is the distance of the boundary from the present position of the particle;

(iii) the distance x to the next collision point is chosen from the distribution $\exp(-\Sigma x)/[1 - \exp(-\Sigma d')]$;

(iv) the weight of the particle is modified by a factor $(\Sigma_s/\Sigma)[1 - \exp(-\Sigma d')]$;

(v) steps (ii) through (iv) are repeated till the particle completes a specified number of collisions.

The integral equation for $M_1(x)$ in this case is also given by Eq. (4). However, the corresponding equation for $M_1^i(x_0)$ is different and can be obtained by a straightforward but lengthy procedure as

$$M_1^i(x_0) = \int_0^1 dR_1 \int_0^1 dR_2 \cdots \int_0^1 dR_i \left[\prod_{j=0}^{i-1} f_j \right] (\Sigma_s/\Sigma)^i (1 - f_i), \tag{13}$$

where

$$f_i = \frac{f_{i-1}(1 - R_i)}{1 - R_i f_{i-1}} \qquad \text{for } i \geqslant 1$$

$$f_i = 1 - \exp[-\Sigma(d - x_0)] \qquad \text{for } i = 0.$$

It may be noted here that the function to be integrated in Eq. (10) is BVHK, whereas that in Eq. (8) is not.

Problem B

In the second problem, we consider the case in which a particle after scattering travels in the same direction with probability α and in an exactly opposite direction with probability $\beta = 1 - \alpha$. Both transmission and reflection from the slab were estimated. Again, the problem was solved in two ways.

The first method, B(1), is basically similar to A(2). However, in this case, the particle direction μ after scattering is sampled from the discrete probability $\alpha\delta_{\mu,\nu}+\beta\delta_{\mu,-\nu}$, where ν is the direction before collision, and both μ and ν take values of $+1$ or -1. The scheme can be described as follows:

(i) the particle starts with $\mu=1$ and $W=1$;

(ii) a score $W\exp(-\Sigma d)$ is given for transmission;

(iii) the distance x to the next collision site is chosen from the distribution $\exp(-\Sigma x)/[1-\exp(-\Sigma d'(\mu))]$, where $d'(\mu)$ is the distance of the particle from the transmission boundary for $\mu=1$ and from the reflection boundary for $\mu=-1$.

(iv) the weight of the particle is modified by a factor $(\Sigma_s/\Sigma)[1-\exp(-\Sigma d(\mu))]$;

(v) a score $[\alpha\delta_{\mu,1}+\beta\delta_{\mu,-1}]\,W\exp[-\Sigma d'(1)]$ for transmission and of $[\alpha\delta_{\mu,-1}+\beta\delta_{\mu,1}]\,W\exp[-\Sigma d'(-1)]$ for reflection is given;

(vi) the particle is allowed to travel in the same direction with probability α; otherwise the direction is reversed.

The expectation value for the transmission satisfies the coupled set of equations

$$M_1(x,1)=\int_x^d dy\Sigma_s\exp[-\Sigma(y-x)][\alpha M_1(y,1)+\beta M_1(y-1)]+\exp[-\Sigma(d-x)] \tag{14a}$$

$$M_1(x,-1)=\int_0^x dy\Sigma_s\exp[-\Sigma(y-x)][\beta M_1(y,1)+\alpha M_1(y,-1)], \tag{14b}$$

where, $M_1(x,\mu)$ is the expected transmission for a particle emitted at x in direction μ. The equations for reflection are of a similar nature.

This coupled set of equations has the solution

$$M_1(\chi,\mu)=A_\mu\exp[-\lambda(d-x)]+B_\mu\exp[\lambda(d-x)], \tag{15}$$

where

$$\lambda=[(\Sigma-\alpha\Sigma_s)^2-\beta^2\Sigma_s^2]^{1/2}$$

$$A_1=\frac{(\Sigma+\lambda-\alpha\Sigma_s)\exp(\lambda d)}{(\Sigma+\lambda-\alpha\Sigma_s)\exp(\lambda d)-(\Sigma-\lambda-\alpha\Sigma_s)\exp(-\lambda d)}$$

$$B_1=\frac{(\Sigma-\lambda-\alpha\Sigma_s)\exp(-\lambda d)}{(\Sigma-\lambda-\alpha\Sigma_s)\exp(-\lambda d)-(\Sigma+\lambda-\alpha\Sigma_s)\exp(\lambda d)}$$

$$A_{-1}=A_1\frac{\Sigma-\lambda-\alpha\Sigma_s}{\beta\Sigma_s}$$

$$B_{-1}=B_1\frac{\Sigma+\lambda-\alpha\Sigma_s}{\beta\Sigma_s}.$$

The equation for $M_1^i(x, \mu)$ for this case can also be worked out in closed form. However, this has not been attempted here, since the procedure is somewhat lengthy and the final expressions do not yield any extra information except that the integrand is BVHK. An infinite series useful for estimating M_1^i for large i is, however, given in Appendix 1. This expression, along with a few numerical experiments, was used to ensure that the truncation error arising due to the termination of the Neumann series after a finite number of terms was negligible.

In B(2), the second method of solving this problem, we have made use of the exponential transform. The exponential transform is a widely used variance reducing technique in deep penetration radiation transport problems [1]. The Monte Carlo scheme remains almost the same as B(1) except that instead of the total cross section Σ, a pseudo cross section $\Sigma^*(\mu) = \Sigma(1 - \mu k)$ is used, where k is a constant $0 \leqslant k \leqslant 1$. The scheme is as follows:

(a) in step (ii), the sampling distribution is changed to $\exp(-\Sigma^*(\mu)\, x/[1 - \exp[-\Sigma^*(\mu)\, d'(\mu)]]$;

(b) in step (iv), the weight modification factor changes to $(\Sigma_s/\Sigma)[1 - \exp[\Sigma^*(\mu)\, d'(\mu)] \exp[-(\Sigma - \Sigma^*(\mu))\, x]$.

The integral equations for $M_1(x, 1)$ and $M_1(x, -1)$ in this case will be exactly the same as in Eq. (11), since the only difference between the two cases is that here we are sampling from an altered distribution.

TABLE I

Maximum and Average Errors for Scheme A1

X_0	Σ	Max. dim.	$N_1 - N_2$	Maximum and average errors for PRS-1	PRS-2	PRS-3	Halton	Faure-1
2	0.5	11	8,000–15,999	1.72-2	1.35-2	3.64-2	2.21-2	2.21-2
				(9.29-3)	(8.10-3)	(2.40-2)	(4.46-3)	(1.75-3)
			16,000–31,999	1.82-2	6.67-3	1.77-2	5.87-3	5.64-3
				(1.28-2)	(1.86-3)	(1.17-2)	(2.15-3)	(4.12-4)
2	0.9	23	8,000–15,999	6.78-3	4.67-3	7.62-3	2.15-3	4.39-3
				(5.23-3)	(2.35-3)	(3.10-3)	(5.04-4)	(5.99-4)
			16,000–31,999	8.08-3	3.59-3	5.20-3	9.61-4	1.82-3
				(5.80-3)	(1.44-3)	(1.11-3)	(4.12-4)	(4.12-4)
5	0.5	23	24,000–47,999	1.46-2	2.77-2	8.24-3	3.49-3	2.05-2
				(4.11-3)	(1.43-2)	(3.00-3)	(1.53-2)	(1.17-2)
			48,000–95,999	8.15-3	3.36-2	1.21-2	1.56-2	2.74-2
				(2.71-3)	(2.73-3)	(3.61-3)	(5.97-3)	(1.64-2)
5	0.9	31	24,000–47,999	6.32-3	1.29-2	1.07-2	5.27-3	9.64-3
				(2.78-3)	(7.30-3)	(4.55-3)	(2.91-3)	(2.76-3)
			48,000–95,999	2.60-3	7.22-3	6.14-3	2.66-3	2.75-3
				(9.38-4)	(5.83-3)	(4.42-3)	(2.17-3)	(1.51-3)

4. Results and Discussions

For integral equations of the type described here, the truncation error may be made arbitrarily small by taking a sufficiently large number of terms in the Neumann series. The solution of the integral equation can therefore be thought of as the evaluation of the sum of a large number of multidimensional integrals. Quasi random sequences are therefore expected to give better convergence asymptotically as $N \to \infty$. In the present study, we attempt to find out how the two types of sequences perform for finite N.

Table I gives the maximum relative error and the average relative error with scheme A(1) for the three PRS and the Halton and the Faure sequences for two different thicknesses (2 and 5 mean free paths (mfp)) and two different scattering probabilities (0.5 and 0.9). Table II gives the same data with scheme A(2) for three different thicknesses (2,5 and 10 mfp).

TABLE II

Maximum and Average Errors for Scheme A2

X_0	Σ	Max. dim.	$N_1 - N_2$	Maximum and average errors for PRS-1	PRS-2	PRS-3	Halton	Faure-1	Faure-2
2	0.5	11	8,000–15,999	3.23-3	3.89-3	3.27-3	2.90-4	5.87-4	—
				(1.90-3)	(2.57-3)	(2.28-3)	(1.54-4)	(2.14-4)	—
			16,000–31,999	2.14-3	2.43-3	2.17-3	1.42-4	2.59-4	—
				(1.33-3)	(8.31-4)	(1.11-3)	(8.28-5)	(1.28-4)	—
2	0.9	11	8,000–15,999	1.06-3	9.45-4	7.27-4	8.32-5	1.56-4	2.84-4
				(6.30-4)	(5.08-4)	(4.58-4)	(5.00-5)	(5.09-5)	(4.49-5)
			16,000-31,999	6.09-4	4.75-4	4.63-4	4.17-5	6.52-5	1.50-4
				(4.13-4)	(9.85-5)	(1.77-4)	(2.42-5)	(2.39-5)	(2.50-5)
5	0.5	11	8,000–15,999	1.02-2	3.20-2	1.99-2	5.48-3	7.69-3	5.14-3
				(5.44-3)	(4.71-3)	(3.34-3)	(1.65-3)	(2.26-3)	(1.00-3)
			16,000–31,999	6.18-3	6.22-3	4.15-3	1.40-3	1.57-3	1.17-3
				(3.76-3)	(2.87-3)	(1.77-3)	(8.57-4)	(8.45-4)	(5.79-4)
5	0.9	17	8,000–15,999	2.29-3	2.42-3	1.88-3	6.57-4	8.77-4	1.31-3
				(1.24-3)	(1.16-3)	(1.08-3)	(3.88-4)	(3.56-4)	(6.30-4)
			16,000–31,999	1.58-3	1.52-3	1.73-3	3.10-4	3.82-4	7.33-4
				(9.94-4)	(9.29-4)	(1.16-3)	(2.07-4)	(1.50-4)	(4.02-4)
10	0.5	17	24,000–47,999	4.01-2	1.21-2	7.16-3	9.04-3	1.36-2	5.23-3
				(2.40-2)	(6.47-3)	(2.47-3)	(6.20-3)	(8.58-3)	(3.17-3)
			48,000–95,999	1.30-2	1.44-2	5.74-3	5.30-3	8.11-3	3.20-3
				(8.37-3)	(9.14-3)	(2.41-3)	(3.29-3)	(3.56-3)	(2.07-3)
10	0.9	23	24,000–47,999	8.92-4	3.05-3	6.71-4	1.35-3	3.97-4	—
				(2.67-4)	(2.10-3)	(2.37-4)	(7.71-4)	(1.91-4)	—
			48,000–95,999	8.74-4	1.82-3	1.04-3	5.82-4	3.91-4	—
				(3.98-4)	(1.04-3)	(5.46-4)	(2.24-4)	(1.56-4)	—

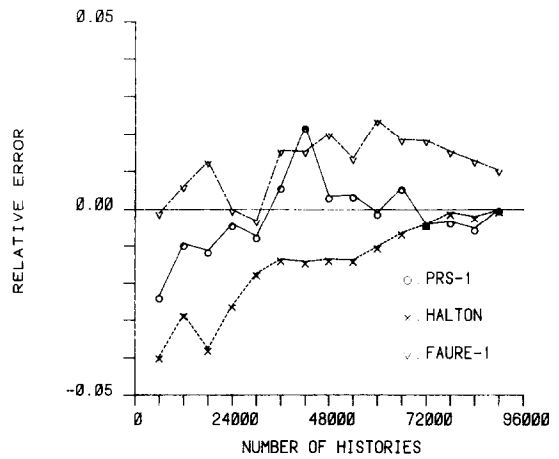

FIG. 1. Relative error with scheme A(1), $d = 5$ mfp, $\Sigma_s/\Sigma = 0.5$.

The maximum relative error in the range of histories N_1 to N_2 is defined as

$$E_{\max}(N_1, N_2) = \sup_{N_1 \leq N \leq N_2} \frac{|I_N - I|}{I}.$$

In a similar manner, the average relative error is defined as

$$E_{\text{av}}(N_1, N_2) = \frac{1}{N_2 - N_1 + 1} \sum_{N=N_1}^{N_2} \frac{|I_N - I|}{I}.$$

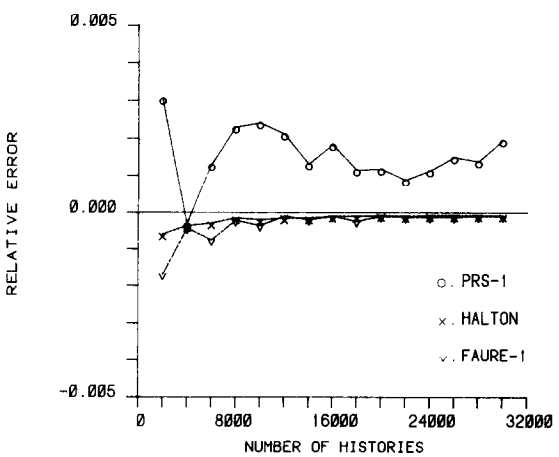

FIG. 2. Relative error with scheme A(2), $d = 2$ mfp, $\Sigma_s/\Sigma = 0.5$.

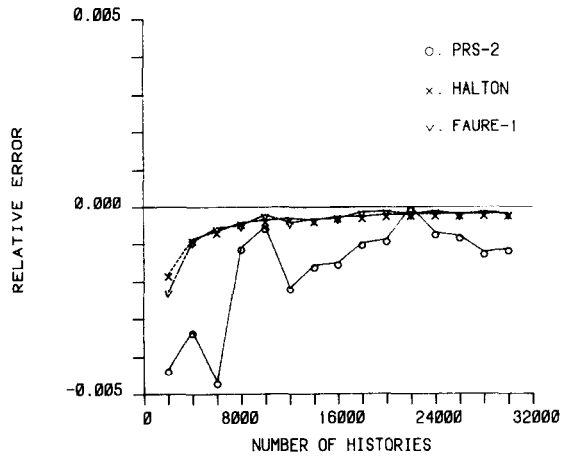

FIG. 3. Relative error with scheme A(2), $d = 5$ mfp, $\Sigma_s/\Sigma = 0.9$.

These two quantities were chosen as measures of the accuracy of the sequence being tested in order to present a large amount of data in a concise manner. Variation of the relative error with the number of histories N for a few representative cases is shown in Figs. 1, 2, and 3 ($d = 5$ mfp, $\Sigma_s/\Sigma = 0.9$, with scheme A(1) in Figs. 1 and 2, scheme A(2) in Fig. 3).

TABLE III

Maximum Relative Error for Individual Collisions with Scheme A2[a]

Collision number[b]	True value	PRS-3	Halton	Faure-1
1 (1)	2.27-4	7.99-2	5.39-2	1.00-1
2 (2)	5.67-4	4.87-2	1.73-2	3.60-1
3 (3)	9.46-4	2.00-2	3.22-3	1.01-2
4 (4)	1.18-3	1.88-2	2.96-3	5.71-3
5 (5)	1.18-3	7.59-3	5.13-3	5.50-3
6 (6)	9.85-4	1.34-2	5.64-3	5.27-3
7 (7)	7.04-4	5.62-3	6.15-3	2.32-3
8 (8)	4.40-4	4.06-3	1.74-3	2.40-3
9 (9)	2.44-4	6.08-3	2.12-3	1.43-3
10(10)	1.22-4	3.71-3	5.06-3	1.22-3
11(11)	5.55-5	4.35-3	3.76-3	1.27-3
12(12)	2.31-5	4.20-3	4.23-3	4.48-3
13(13)	8.90-6	7.75-3	2.62-3	3.55-3
14(14)	3.18-6	5.36-3	4.51-3	2.20-3

[a] Slab thickness = 10 mfp, $\Sigma_s = 0.5$, $N_1 = 48{,}000$, $N_2 = 95{,}999$.
[b] Values in parentheses are the dimensionality of the integral.

From Table I, we see that for scheme A(1), the QRS seem to be a bit better than the PRS for 2 mfp, whereas the PRS are a bit better for 5 mfp. However, no clear conclusion can be drawn since the variation among the PRS themselves is more than the variation between the PRS and the QRS.

For scheme A(2), on the other hand (Table II), both the Halton and the Faure sequences appear to be distinctly superior to the PRS in the range of histories studied for 2 and 5 mfp. The maximum relative error in the range 16,000–31,999 is less than that for the best PRS by factors ranging from 3 to 15. Even for 10 mfp, with $\Sigma_s = 0.5$, the QRS are better than two of the PRS (PRS-1 and PRS-2). Further, for PRS-3, which gave comparable accuracy, a collision by collision analysis showed that this was due to an accidental cancelation of errors (see Table III). For most of the collisions which make significant contributions to the final result, the QRS seem to be distincly superior.

The major reason why the QRS perform better with scheme A(2) then with A(1) is that for the same collision, the dimensionality in A(2) is less than that in A(1) by a factor of approximately 2— the ith collided flux in A(1) involves $2i+1$ dimensions, whereas it involves only i dimensions in A(2). In general, for BVHK functions, QRS begin to outperform PRS only beyond a certain number of histories, this number increasing rapidly with dimensionality. This is because as the dimensionality increases, the effect of the term $(\log N)^s$ in the discrepancy of the QRS is more pronounced for small N. For large N, this factor becomes insignificant and the discrepancy decreases as $1/N$.

TABLE IV

Maximum Relative Errors for Individual Collisions with Scheme A2[a]

Collision number[b]	True value	PRS-3	Halton	Faure-1
1 (1)	3.03-2	1.14-2	3.85-3	8.77-3
2 (2)	6.82-2	2.09-2	1.71-3	3.37-3
3 (3)	1.02-1	8.56-3	1.17-3	2.86-3
4 (4)	1.15-1	6.27-3	1.03-3	2.71-3
5 (5)	1.04-1	5.66-3	9.13-4	2.49-3
6 (6)	7.77-2	8.42-3	1.82-3	2.01-3
7 (7)	5.00-2	7.37-3	2.28-3	2.43-3
8 (8)	2.81-2	1.96-2	4.59-3	4.82-3
9 (9)	1.41-2	2.79-2	8.35-3	1.17-2
10(10)	6.32-3	3.05-2	7.26-3	7.84-3
11(11)	2.59-3	3.54-2	2.92-2	1.30-2
12(12)	9.70-4	4.22-2	2.39-2	4.42-2
13(13)	3.76-4	8.76-2	7.87-2	6.20-2
14(14)	1.08-4	6.87-2	2.11-1	1.44-1
15(15)	3.24-5	9.61-2	1.78-1	3.32-1

[a] Slab thickness 5 mfp, $\Sigma = 0.9$, $N_1 = 16{,}000$, $N_2 = 31{,}999$.

[b] Values in parentheses refer to dimensionality of the integral.

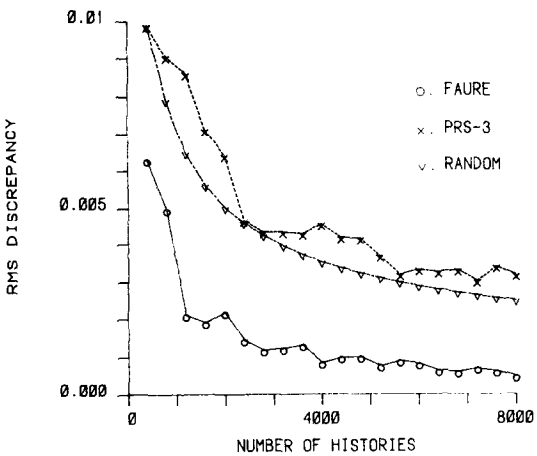

FIG. 4. RMS discrepancy for PRS-3 and Faure sequence for $s = 4$.

The effect of dimensionaliy can be seen in Tables III and IV, where the maximum relative error for one PRS and the Halton and the Faure sequences is shown for different collisions. The relative performance of the QRS is better for smaller dimensions except for a few accidental fluctuations.

The effect of dimensionality can also be seen in Figs. 4 and 5, which are plots of the RMS discrepancy against N for PRS-3 and the Faure sequence for dimensions 4 and 10, respectively. These were obtained using Warnock's method [12]. For the sake of comparison, the expectation value of the RMS discrepancy of a random sequence (see Eq. (2)) has also been plotted in the same graphs. For $s = 4$, the dis-

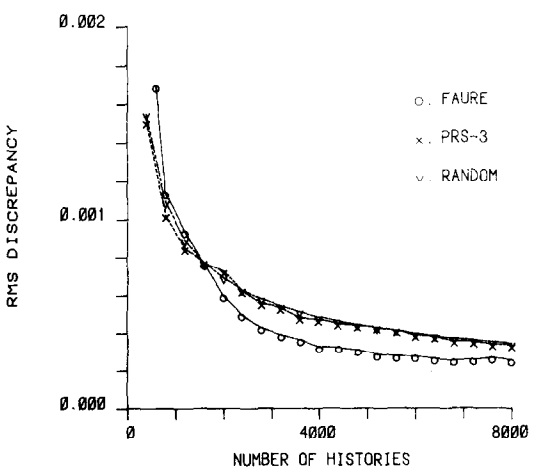

FIG. 5. RMS discrepancy for PRS-3 and Faure sequence for $s = 10$.

crepancy of the Faure seqeunce is lower than that of the PRS for all N, whereas for $s = 10$, the discrepancy slowly starts becoming better only for $N > 2000$.

The fact that the functions encountered in scheme A(1) are not of BVHK may also have contributed to the relatively poorer performance of the QRS with this scheme. It may be noted here that all the theorems predicting the errors of the use of QRS for integration assume that the integrand is BVHK. On the other hand, for a random sequence (which the PRS may be expected to approximate), one would still get an error to be $O(1/\sqrt{N})$ asymptotically with scheme A(1) since the non-BVHK functions in A(1) are products of theta functions.

To check this a little further, a few results were obtained with a scheme which we designate A(1)′. This scheme was similar to A(1) in all respects except that the particle was not killed at every collision with probability $(1 - \Sigma_s/\Sigma)$; instead its weight was modified by a factor Σ_s/Σ (survival biasing). With this procedure, the dimensionality of the problem becomes almost equal to that with A(2), without in any way changing the non BVHK nature of the integrand. (For this scheme, the ith collided flux is evaluated by means of a $i+1$ dimensional integral.) Table V gives a comparison of the ratios of the maximum relative error of the PRS and the Halton sequence with schemes A(1)′ and A(2) for a few cases. In almost all the cases, the relative performance of the Halton sequence was appreciably better with A(2) than with A(1)′. Though not conclusive, this lends support to the view that the QRS

TABLE V

Ratio of the Maximum Relative Errors between PRS and Halton Sequences for Non BVHK[a] and BVHK Functions

			Ratio of maximum relative errors					
			PRS-1/Halton		PRS-2/Halton		PRS-3/Halton	
X_0	Σ_s	N_1–N_2	NBVHK	BVHK	NBVHK	BVHK	NBVHK	BVHK
2	0.5	4,000–7,999	2.00	2.46	3.31	6.23	3.47	5.08
		8,000–15,999	3.81	11.13	7.71	13.41	7.72	11.28
		16,000–31,999	5.26	14.56	2.88	16.53	7.14	14.56
2	0.9	4,000–7,999	2.10	2.09	2.22	5.04	2.67	2.76
		8,000–15,999	3.36	12.74	3.44	11.36	4.92	8.74
		16,000–31,999	5.27	14.60	1.54	11.39	4.81	11.10
5	0.5	4,000–7,999	1.08	1.86	1.03	5.84	1.79	3.63
		8,000–15,999	1.37	3.62	1.47	4.40	2.78	2.63
		16,000–31,999	1.87	4.41	2.17	4.44	2.96	2.96
5	0.9	4,000–7,999	0.72	4.03	0.75	3.60	2.29	2.01
		8,000–15,999	1.66	3.49	1.16	3.68	2.84	2.86
		16,000–31,999	2.37	5.10	1.40	4.90	1.54	5.58

[a] NBVHK refers to scheme A1′, which combines analog sampling of collision points and leakage with survival biasing.

may perform better with BVHK functions than with the type of non BVHK functions encountered in scheme A(1).

Now, we try to compare the performance of the sequences among themselves. So far as the PRS are concerned, there are considerable variations among themselves in each individual case. On the whole, however, none of the sequences can be considered to be clearly superior for problems of this type.

Between the Halton and the Faure sequences, the Halton sequence performs as well as, and in many cases better than, the Faure sequence. This result, at first sight, appears surprising since the constant C_s in the theoretical bounds on the discrepancy tends to ∞ with s for the Halton sequence and to 0 for the Faure sequence (Eqs. (3), (4), (5) and (6)). A likely explanation for this behaviour is provided by the fact that the Faure-1 sequence was generated with a single prime corresponding to the largest dimensionality integral encountered in the problem, i.e., for a problem in which the largest dimensionality integral was 11, the prime used was 11 and all the lower dimensional integral were also evaluated using the same sequence. As is evident from Eq. (6), such a procedure leads to large discrepancies for lower dimensional integrals. Some results were also obtained using the most optimal prime for each collision (Faure-2). In general, the errors decreased with the use of Faure-2, but since the errors themselves are small, the

TABLE VI

Maximum and Average Errors with Scheme B1 for a 2 mfp Slab

Σ	Max. dim.	T/R[a]	$N_1 - N_2$	Maximum and average errors for PRS-1	PRS-2	PRS-3	Halton	Faure-1	Faure-2
0.5	23	T	8,000–15,999	2.02-3	2.97-3	2.59-3	3.60-4	1.20-3	4.72-4
				(9.65-4)	(1.51-3)	(1.18-3)	(1.50-4)	3.30-4)	(2.18-4)
			16,000–31,999	2.16-3	1.53-3	1.06-3	1.89-4	5.18-4	2.47-4
				(1.59-3)	(9.82-4)	(7.03-4)	(1.07-4)	(1.40-4)	(1.09-4)
0.5	23	R	8,000–15,999	6.30-3	3.28-3	3.37-3	5.21-4	3.54-3	6.20-4
				(4.05-3)	(1.57-3)	(1.08-3)	(1.91-4)	(1.26-3)	(2.43-4)
			16,000–31,999	5.23-3	2.65-3	3.24-3	2.74-4	1.54-3	3.14-4
				(4.01-3)	(1.10-3)	(1.90-3)	(1.27-4)	(4.46-4)	(1.22-4)
0.9	23	T	8,000–15,999	2.28-3	5.70-3	2.60-3	9.89-4	6.42-3	1.11-3
				(9.69-4)	(3.53-3)	(5.85-4)	(5.86-4)	(2.75-3)	(6.82-4)
			16,000–31,999	2.43-3	2.90-3	1.93-3	9.65-4	2.76-3	7.36-4
				(1.53-3)	(2.24-3)	(7.04-4)	(7.10-3)	(1.32-3)	(3.90-4)
0.9	23	R	8,000–15,999	7.59-3	2.19-3	6.24-3	7.49-4	8.47-3	1.94-3
				(5.24-3)	(7.18-4)	(3.89-3)	(1.54-4)	(2.67-3)	(7.67-4)
			16,000–31,999	6.59-3	1.46-3	3.94-3	4.72-4	2.98-3	7.94-4
				(4.83-3)	(4.84-4)	(1.13-3)	(1.95-4)	(9.43-4)	(3.92-4)

[a] T—transmission; R—reflection.

effect is not very pronounced. The improvement obtained with Faure-2 was more pronounced for problem B and is discussed later.

A few cases were also studied using the scrambled Halton sequence. In all the cases studied, however, the scrambled Halton sequence was only marginally better. For example, for a 2 mfp slab with $\Sigma_s = 0.5$ using scheme A(2), the maximum relative error was 1.47–4 with the Halton sequence and 1.40–4 with the scrambled Halton sequence. Similarly, for a 2 mfp slab with $\Sigma_s = 0.9$ using scheme A(2), the maximum error with the Halton sequence was 4.17–5 and with the scrambled Halton sequence, it was 3.43-5. The range of histories in both the cases was 16,000–31,999.

Tables VI through IX give the maximum and average relative errors for both the transmitted and the reflected fluxes at the boundaries of the slab for the straight ahead and back case (problem B) for 2 and 5 mfp. This problem may be considered to be [illegible] physical problems. The Halton sequence is clearly superior to thicknesses. The same result is illustrated by Figs. 6 through 9, which are plots of the relative error against the number of histories for a few representative cases. Faure-1, however, does not perform very well. Faure-2 performs about as well as the Halton sequence. It is not clear as to why the Faure sequence did not outperform the Halton sequence despite using the most optimal primes for each integral.

TABLE VII

Maximum and Average Errors with Scheme B1 for a 5 mfp Slab

Σ	Max. dim.	T/R[a]	$N_1 - N_2$	Maximum and average errors for PRS-1	PRS-2	PRS-3	Halton	Faure-1	Faure-2
0.5	31	T	8,000–15,999	1.54-2	1.87-2	2.26-2	5.28-3	1.77-2	3.00-3
				(1.08-2)	(1.40-2)	(1.75-2)	(2.60-3)	(6.87-3)	(7.52-3)
			16,000–31,999	1.25-2	1.88-2	1.87-2	2.65-3	1.02-2	2.17-3
				(9.27-3)	(1.39-2)	(1.66-2)	(1.59-3)	(4.96-3)	(7.75-4)
0.5	31	R	8,000–15,999	1.18-2	5.22-3	4.69-3	9.07-4	5.34-3	9.47-4
				(1.00-2)	(3.63-3)	(4.06-3)	(3.45-4)	(2.40-3)	(3.63-4)
			16,000–31,999	1.16-2	6.30-3	5.12-3	4.23-4	3.05-3	4.25-4
				(9.68-3)	(5.35-3)	(4.52-3)	(2.05-4)	(7.36-4)	(9.88-5)
0.9	48	T	8,000–15,999	1.25-2	8.32-3	9.35-3	9.47-3	5.29-2	—
				(5.16-3)	(4.25-3)	(1.87-3)	(4.23-3)	(3.02-2)	—
			16,000–31,999	7.82-3	8.72-3	7.14-3	5.61-3	5.36-2	—
				(1.58-3)	(2.82-3)	(3.57-3)	(3.62-3)	(4.46-2)	—
0.9	49	R	8,000–15,999	7.14-3	5.61-3	7.91-3	2.86-3	2.90-2	—
				(5.43-3)	(3.66-3)	(5.23-3)	(1.21-3)	(4.40-3)	—
			16,000–31,999	5.74-3	3.41-3	3.01-3	1.30-3	1.46-2	—
				(4.16-3)	(6.04-4)	(1.98-3)	(6.51-4)	(8.93-3)	—

[a] T—transmission; R—reflection.

TABLE VIII

Maximum and Average Errors with Scheme B2 for a 2 mfp Slab[a]

Σ	Max. dim.	T/R[b]	$N_1 - N_2$	Maximum and average errors for PRS-1	PRS-2	PRS-3	Halton	Faure-1	Faure-2
0.5	23	T	8,000–15,999	8.44-4	8.64-4	1.14-3	1.05-4	1.62-3	1.92-4
				(3.33-4)	(3.75-4)	(5.07-4)	(2.98-4)	(6.04-4)	(4.71-5)
			16,000–31,999	4.52-4	6.10-4	8.25-4	5.61-5	6.27-4	8.16-5
				(1.42-4)	(2.49-4)	(3.71-4)	(1.17-5)	(2.35-4)	(1.63-5)
0.5	23	R	8,000–15,999	1.21-2	6.77-3	6.98-3	5.12-4	3.84-3	7.77-4
				(8.79-3)	(4.03-3)	(3.00-3)	(1.32-4)	(1.85-3)	(2.62-4)
			16,000–31,999	9.09-3	5.92-3	9.03-3	3.45-4	1.94-3	2.83-4
				(7.49-3)	(2.34-3)	(5.73-3)	(1.07-4)	(4.71-4)	(7.84-5)
0.9	23	T	8,000–15,999	2.37-3	3.80-3	3.54-3	7.34-4	6.85-3	6.93-4
				(7.53-4)	(2.41-3)	(1.82-3)	(3.93-4)	(3.20-3)	(1.88-4)
			16,000–31,999	1.22-3	2.54-3	2.36-3	7.78-4	2.95-3	4.49-4
				(3.96-4)	(1.70-3)	(1.02-3)	(5.56-4)	(1.61-3)	(1.92-4)
0.9	23	R	8,000–15,999	1.03-2	3.70-3	6.75-3	7.92-4	7.47-3	2.45-3
				(7.44-3)	(1.29-3)	(3.46-3)	(2.27-4)	(2.93-3)	(9.74-4)
			16,000–31,999	8.38-3	2.59-3	3.69-3	6.32-4	3.08-3	7.16-4
				(6.68-3)	(8.55-4)	(1.41-3)	(2.55-4)	(8.31-4)	(1.65-4)

[a] Biasing parameter k is 0.67 for $\Sigma_s = 0.5$ and 0.29 for $\Sigma_s = 0.9$.
[b] T—transmission; R—reflection.

TABLE IX

Maximum and Average Errors with Scheme B2 for a 5 mfp Slab[a]

Σ	Max. dim.	T/R[b]	$N_1 - N_2$	Maximum and average errors for PRS-1	PRS-2	PRS-3	Halton	Faure-1	Faure-2
0.5	31	T	8,000–15,999	5.52-3	6.87-3	4.98-3	1.31-3	2.24-2	4.15-3
				(1.80-3)	(2.01-3)	(2.25-3)	(6.70-4)	(1.25-2)	(2.35-3)
			16,000–31,999	1.75-3	2.76-3	3.55-3	8.08-4	9.44-3	2.17-3
				(6.27-4)	(1.23-3)	(1.11-3)	(3.38-4)	(5.71-3)	(1.23-3)
0.5	31	R	8,000–15,999	2.85-2	2.51-2	2.29-2	1.88-3	3.43-2	5.19-3
				(2.21-2)	(1.71-2)	(1.58-2)	(5.66-4)	(1.68-2)	(2.84-3)
			16,000–31,999	2.39-2	1.33-2	2.11-2	1.11-3	1.28-2	1.87-3
				(1.77-2)	(6.77-3)	(9.21-3)	(3.12-4)	(9.86-3)	(1.16-3)
0.9	49	T	8,000–15,999	1.54-2	8.90-3	9.86-3	4.11-3	7.63-2	—
				(9.75-3)	(4.46-3)	(2.03-3)	(1.46-3)	(6.14-2)	—
			16,000–31,999	1.32-2	5.33-3	4.54-3	2.52-3	6.73-2	—
				(4.24-3)	(2.08-3)	(2.12-3)	(1.08-3)	(4.26-2)	—
0.9	49	R	8,000–15,999	8.60-3	4.53-3	1.61-2	3.97-3	1.23-1	—
				(5.47-3)	(1.98-3)	(1.01-2)	(1.18-3)	(6.39-2)	—
			16,000–31,999	1.01-2	5.05-3	3.88-3	1.11-3	3.08-2	—
				(7.85-3)	(2.44-3)	(2.04-3)	(4.11-4)	(2.08-2)	—

[a] Biasing parameter k is 0.67 for $\Sigma_s = 0.5$ and 0.29 for $\Sigma_s = 0.9$.
[b] T—transmission; R—reflection.

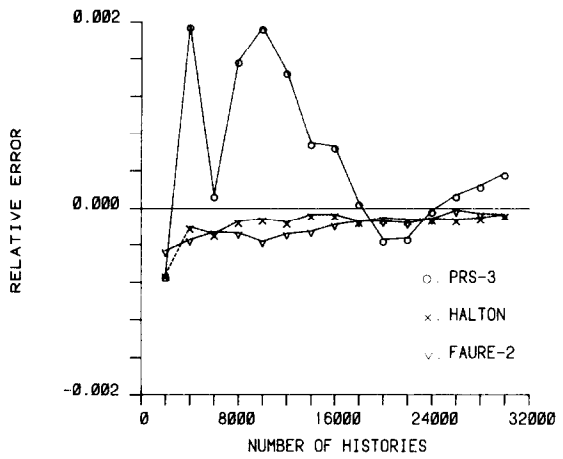

FIG. 6. Relative error in transmission with scheme B(1), $d = 2$ mfp, $\Sigma_s/\Sigma = 0.5$, $\alpha = 0.6$.

It may be noted here that the use of the Faure sequence in this manner takes considerably more computer time—e.g., for a 23 dimensional problem, 100 random numbers have to be generated. Therefore, it seems that for problems of this type the most optimal use of the Faure sequence would be with the judicious use of a few primes.

No attempt was made to compare the efficiencies of the different sequences, which would have involved the estimation of the computation time per history also. This was because the relative importance of the generation time for any sequence will greatly depend on the type of problem studied. However, as one would expect, the QRS take much more computing time than the PRS.

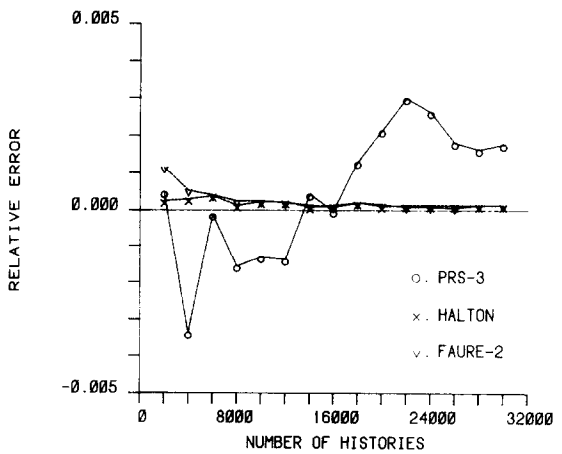

FIG. 7. Relative error in reflection with scheme B(1), $d = 2$ mfp, $\Sigma_s/\Sigma = 0.5$, $\alpha = 0.6$.

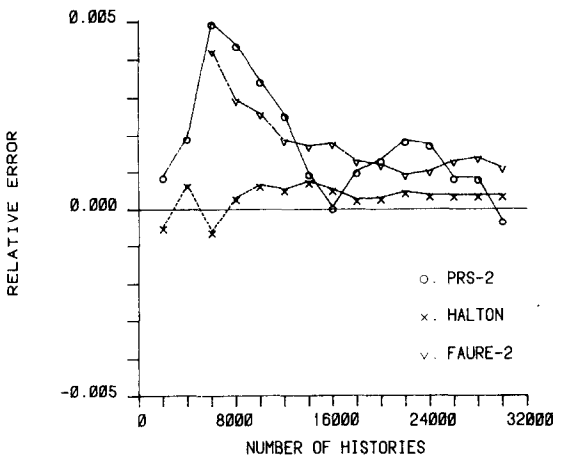

FIG. 8. Relative error in transmission with scheme B(2), $d = 5$ mfp, $\Sigma_s/\Sigma = 0.5$, $\alpha = 0.6$, bias parameter $k = 0.67$.

Just as we had completed the revision of our manuscript, we received a preprint of a paper by Bennett L. Fox on the implementation and efficiency of quasi random generators [13]. In this paper, the efficiencies of the Halton, Faure and Sobol sequences and a pseudo random sequence are compared for test multidimentional integrals. The conclusions are that the Sobol sequence is to be preferred for dimensions 2 through 6 and the Faure sequence for dimensions larger than 6. The latter conclusion differs somewhat from ours. We believe the difference may be mainly due to the difference in the type of problem studied—we consider an integral equation, whereas they consider a multidimensional integral.

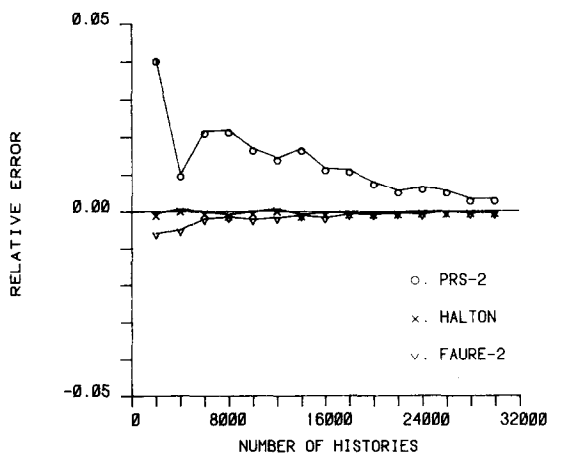

FIG. 9. Relative error in reflection with scheme B(2), $d = 5$ mfp, $\Sigma_s/\Sigma = 0.5$, $\alpha = 0.6$, bias parameter $k = 0.67$.

CONCLUSIONS

1. The QRS yield higher accuracies when the errors themselves are small and therefore may be useful in high precision work in radiation transport such as in benchmark problems.

2. As expected on theoretical grounds, the performance of the QRS is better when the dimensionality of the problem is small. Smaller dimensions are associated with small thicknesses as well as Monte Carlo schemes which make use of procedures such as survival biasing, expectation estimator, etc.

3. For the kind of problems studied here, the Halton and the Faure sequences perform equally well. No appreciable advantage was obtained with the use of scrambled Halton sequences.

4. Though not conclusive, it appears that the relative performance of the QRS is poorer with analog schemes which give rise to non BVHK functions.

APPENDIX 1

We consider a slab of thickness d mfp and with Σ and Σ_s as the total and scattering cross sections, respectively. Let, $\psi_1(X, n)$ and $\psi_2(X, n)$ be the nth scattered forward and backward fluxes at x, respectively. They, then, satisfy the equations

$$(-1)^{i+1}\frac{d\psi_i(x,n)}{dx}+\Sigma\,\psi_1(x,n)=\Sigma_s[\alpha\psi_i(x,n-1)+\beta\psi_{3\ \ i}(x,n-1)],$$
$$i=1,2;\ n\geqslant 1$$
$$\psi_i(X,0)=\exp(-\Sigma x)\,\delta_{i,1}$$

subject to the boundary conditions

$$\psi_1(0,n)=0, \qquad n=1,2,\ldots$$
$$\psi_2(d,n)=0, \qquad n=1,2,\ldots.$$

To separate the variables, we express $\psi_i(x, n)$ as

$$\psi_i(x,n)=\sum_{k=0}^{\infty}A_k(n)\,\phi_{i,k}(x)$$

and obtain for $A_k(n)$ and $\phi_{i,k}(x)$, the expressions

$$(-1)^{i+1}\frac{d\phi_{i,k}(x)}{dx}+\Sigma(1-\alpha\Sigma_s\lambda_k)\,\phi_{i,k}(x)=\beta\lambda_k\Sigma_s\phi_{3-i,k}(x)$$

and

$$\lambda_k A_k(n)=A_k(n-1).$$

Using standard procedures (see, for example, Davison [14]), i.e, writing the corresponding equations for the adjoint fluxes and making use of orthogonality relations, we can obtain the complete solution for the fluxes. Since our interest, however, is only with large n, we give below the solutions corresponding to the smallest eigenvalue λ_0

$$\phi_{1,0}(x) = \sin \omega_0 x$$
$$\phi_{2,0}(x) = \sin \omega_0 (d - x)$$
$$A_0(n) = (\Sigma_s / \Sigma \lambda_0)^n \, c(\alpha c_1 + \beta c_2),$$

where λ_0 and ω_0 are obtained as solutions of the equations

$$-(1 - \alpha\lambda_0)^2 + \beta^2 \lambda_0^2 = \omega_0^2$$

and

$$\exp(-2i\omega_0 d) = \frac{-i\omega_0 + 1 - \alpha\lambda_0}{i\omega_0 + 1 - \alpha\lambda_0}$$

and c, c_1 and c_2 are given by

$$c = \frac{2\gamma}{2\alpha(\sin \gamma d - \gamma d \cos \gamma d) + \beta(2d - \sin 2\gamma d)}$$
$$c_1 = \frac{\Sigma \sin \gamma d - \gamma \cos \gamma d + \gamma \exp(-\Sigma d)}{\Sigma^2 + \gamma^2}$$
$$c_2 = \frac{\gamma - \exp(-\Sigma d)(\Sigma \sin \gamma d + \gamma \cos \gamma d)}{\Sigma^2 + \gamma^2}.$$

ACKNOWLEDGMENTS

We thank Dr. Harald Niederreiter for suggesting the parameters used with PRS-2 and PRS-3 and for other useful suggestions. We thank Dr. Henri Faure for sending us the permutations used in scrambling the Halton sequence and for valuable suggestions. We thank Professor Bennett Fox for useful correspondence.

REFERENCES

1. J. M. HAMMERSLEY AND D. C. HANDSCOMB, Monte Carlo Methods (Methuen, London, 1964), p. 97.
2. E. BRAATEN AND G. WELLER, *J. Comput. Phys.* **33**, 249 (1979).
3. G. MARSAGLIA, *in* "Application of Number Theory to Numerical Analysis," edited by S. K. Zaremba (Academic Press, New York, 1972).
4. H. NIEDERREITER, *Bull. Am. Math. Soc.* **84**, No. 6, 957 (1978).
5. J. H. HALTON, *in* "Application of Number Theory to Numerical Analysis, edited by S. K. Zaremba (Academic Press, New York, 1972).

6. L. K. HUA AND Y. WANG, Application of Number Theory to Numerical Analysis (Springer–Verlag, Berlin, 1981).
7. I. BOROSCH AND H. NIEDERREITER, *BIT* **23**, No. 1, 65 (1983).
8. J. H. HALTON, *Numer. Math.* **2**, 84 (1960).
9. H. FAURE, *Acta Arith.* **41**, 337 (1982).
10. H. FAURE, *Bull. Soc. Math. France* **109**, No. 2, 142 (1981).
11. H. FAURE, UER de Mathematique, Université de Provence, Marseille, France, private communication (1985).
12. T. WARNOCK, *in* "Application of Number Theory to Numerical Analysis, edited by S. K. Zaremba, (Academic Press, New York, 1972).
13. B. L. FOX, Department of Computer Science, University of Montreal, to be published (1986).
14. B. DAVISON, Neutron Transport Theory (Oxford Univ. Press, London, 1957), p. 28.